



Published in final edited form as:

J Cell Sci. 2005 January 15; 118(Pt 2): 433–446.

Neurite extension in central neurons: a novel role for the receptor tyrosine kinases Ror1 and Ror2

Sabrina Paganoni and Adriana Ferreira*

Department of Cell and Molecular Biology, Feinberg School of Medicine and Institute for Neuroscience, Northwestern University, Chicago, IL 60611, USA

Summary

Neurite elongation and branching are key cellular events during brain development as they underlie the formation of a properly wired neuronal network. Here we report that the receptor tyrosine kinases Ror1 and Ror2 modulate the growth of neurites as well as their branching pattern in hippocampal neurons. Upon Ror1 or Ror2 suppression using antisense oligonucleotides or RNA interference (RNAi), neurons extended shorter and less branched minor processes when compared to those in control cells. In addition, Ror-depleted cells elongated longer, albeit less branched, axons than seen in control cells. Conversely, Ror overexpression both in non-neuronal cells and in hippocampal neurons resulted in the enhanced extension of short and highly branched processes. These phenotypes were accompanied by changes in the microtubule-associated proteins MAP1B and MAP2. Taken together, these results support a novel role for Ror receptors as modulators of neurite extension in central neurons.

Keywords

Receptor tyrosine kinases; Antisense; siRNA; Neurite elongation and branching; Microtubule-associated proteins

Introduction

Neuronal terminal differentiation is characterized by the elongation of axons and dendrites, two types of neuritic processes with distinct morphology, molecular composition and function (reviewed by Craig and Banker, 1994). The formation of these specialized cytoplasmic domains depends on the interaction of external cues and intracellular mechanisms. Components of the extracellular matrix, cell adhesion molecules and soluble factors such as neurotrophins, are among the extracellular cues that modulate the direction and extent of neurite growth. Microtubules and actin filaments, on the other hand, are key players in the intracellular mechanisms leading to the elongation of neuronal projections.

The molecular mechanisms underlying the interplay between these extracellular signals and cytoskeletal elements have not been completely elucidated (Tanaka and Sabry, 1995; Skaper et al., 2001; Dickson, 2002). However, a growing body of evidence indicates that the first step in the transduction of guidance cues into neurite growth occurs at the level of the cell membrane. Several studies suggest that a complex array of receptors, mainly receptor tyrosine kinases (RTKs), transmits environmental information to specific intracellular signaling pathways (Mueller, 1999; Schlessinger, 2000; Klein, 2001; Skaper et al., 2001; Huang and Reichardt,

*Author for correspondence (e-mail: a-ferreira@northwestern.edu).

Supplementary material available online at <http://jcs.biologists.org/cgi/content/full/118/2/433/DC1>

2003). Recently, Ror1 and Ror2, members of a new family of RTKs, have been added to the list of potential receptors implicated in the terminal differentiation of central neurons (Masiakowski and Carroll, 1992; Wilson et al., 1993; Oishi et al., 1997; Forrester et al., 1999; Koga et al., 1999; Oishi et al., 1999; McKay et al., 2001; Hikasa et al., 2002).

Although very little is known about Ror1 and Ror2 function, their pattern of expression and subcellular localization suggests a role for these RTKs during neurite elongation in mammalian central neurons. Thus, Ror expression coincides with periods of active neurite extension both in vitro and in vivo (Oishi et al., 1999; Al-Shawi et al., 2001; McKay et al., 2001; Paganoni and Ferreira, 2003). Furthermore, in hippocampal neurons, Ror proteins are highly expressed in actively growing neurites and are concentrated at the leading edge of the growth cones, a cellular compartment that is home to a variety of molecules that control the rate and direction of growth (Paganoni and Ferreira, 2003). However, the perinatal lethality of Ror1 and Ror2 knockout mice has prevented the analysis of the neurological abnormalities that may accompany Ror protein genetic manipulations in vivo (Yoda et al., 2003). As a consequence, no evidence regarding the role of Ror1 and Ror2 in the developmental events that lead to the formation of the mammalian central nervous system is available.

To obtain direct evidence of the role of Ror1 and/or Ror2 in the signaling pathways involved in neurite elongation, we performed a series of loss- and gain-of-function experiments in cultured hippocampal neurons. Our results showed that the genetic knockdown of Ror proteins using antisense oligonucleotides and RNA interference (RNAi) led to the elongation of shorter minor neurites but longer axons than in control hippocampal neurons. In addition, neurite branching in both types of processes was decreased. Conversely, the overexpression of these RTKs in hippocampal neurons, as well as in other non-neuronal cell types, resulted in the extension of short and highly branched neuritic processes. Our results also suggest that these phenotypes could be mediated, at least in part, by changes in the expression levels of the microtubule-associated proteins MAP1B and MAP2. Together, these data indicate that Ror1 and Ror2 play an important role in modulating neurite growth in central neurons.

Materials and Methods

Preparation of hippocampal cultures

Neuronal cultures were prepared from the hippocampi of embryonic day 16 (E16) mouse embryos as previously described (Goslin and Banker, 1991). In brief, embryos were removed and their hippocampi dissected and freed of meninges. The cells were dissociated by trypsinization (0.25% for 15 minutes at 37°C) followed by trituration with a fire-polished Pasteur pipette and plated onto poly-L-lysine-coated coverslips or 60 mm tissue culture dishes in minimum essential medium (MEM) with 10% horse serum. Coverslips were then transferred to dishes containing an astroglial monolayer and maintained in MEM containing N2 supplements (Bottenstein and Sato, 1979) plus ovalbumin (0.1%) and sodium pyruvate (0.1 mM). For biochemical experiments, the medium was replaced with gliaconditioned MEM containing N2 supplements (Bottenstein and Sato, 1979) plus ovalbumin (0.1%) and sodium pyruvate (0.1 mM).

Cell lines

Human embryonic kidney (HEK293) cells were maintained in Minimum Essential Medium (MEM) plus 10% horse serum (Invitrogen, Carlsbad, CA) and grown at 37°C in 5% CO₂ and 90% humidity. Cultures were fed twice a week and passaged when 80% confluent. Cells were renewed every ten passages.

Antisense treatments

Oligonucleotides were designed to target the 5' end of the mouse Ror1 and Ror2 cDNAs and were synthesized by Biosource International (Camarillo, CA). The following 18-mer antisense oligonucleotides were used in this study: Ror1, 5'-CTGTTTCTTGGGCATCAG-3' and Ror2, 5'-CACAGAGGCACACGGCTC-3', corresponding to nucleotides 80–97 and 24–41 of the Ror1 and Ror2 mouse cDNAs, respectively (Oishi et al., 1999). Controls were treated with sense oligonucleotides (Ror1, 5'-CTGATGCCCAAGAAACAG-3' and Ror2, 5'-GAGCCGTGTGCCTCTGTG-3'). All oligonucleotides contained phosphorothioate groups at the final three residues in the 3' terminal region (Ferreira, 1999).

Sense and antisense oligonucleotides were added 2 hours after plating (plating density: 75,000 cells/dish) directly to the culture media at a 50 μ M final concentration. In dose-response experiments, oligonucleotide concentrations ranged from 12 μ M to 50 μ M. Treatments were repeated every 12 hours by adding the oligonucleotides at half the initial final concentration. Cells were analyzed 24–48 hours after plating.

siRNA preparation and transfection

Twenty-one-mer siRNAs corresponding to Ror1 and Ror2 were designed with two-base overhangs on each strand using Qiagen software (Elbashir et al., 2001b). The following target sequences were used: Ror1, 5'-AATCTCCTTCCGGGCAACCAA-3' and Ror2, 5'-AAGATTCGGAGGCAATCGACA-3', corresponding to nucleotides 312–332 and 107–127 of the Ror1 or Ror2 mouse cDNAs, respectively (Oishi et al., 1999). As controls, scrambled siRNAs ('siRNA SCR') and siRNAs carrying a two-base pair change ('siRNA MUT') were used (Ror1-SCR, 5'-AACCTGCGACCTAGCTCCTAA-3'; Ror2-SCR, 5'-AATGTCACAGATAAGCGAGCG-3'; Ror1-MUT, 5'-AATCTCCTTCCGAACAACCAA-3'; Ror2-MUT, 5'-AAGATTCGGAAACAATCGACA-3'). As an additional negative control, siRNA targeting a non-mammalian gene was used ('Non-specific siRNA'). This siRNA is directed against the section 21/136 of the complete genome of *Thermotoga maritima* (Qiagen) (Elbashir et al., 2001a; Krichevsky and Kosik, 2002). siRNAs were chemically synthesized and annealed for duplex formation by Qiagen (Germantown, MD).

Transfections were carried out in 60 mm tissue culture dishes 2 hours after plating (plating density: 250,000 cells/dish) using the TransMessenger transfection reagent (Qiagen). 3 μ g siRNA, 6 μ l Enhancer R and 15 μ l TransMessenger reagent per dish were used. The transfection complex was diluted in warm MEM containing N2 supplements to a final concentration of 100 nM and was added directly to the cultures. After a 3-hour incubation, hippocampal cultures were rinsed in warm MEM and then maintained in glia-conditioned MEM containing N2 supplements (Bottenstein and Sato, 1979) plus ovalbumin (0.1%) and sodium pyruvate (0.1 mM). Cells were analyzed 24–48 hours later. In dose-response experiments, siRNA duplex concentrations ranged from 1 nM to 100 nM.

Some experiments (western blot analysis of Ror2 downregulation by RNAi) were then repeated using the Nucleofector™ apparatus (Amaxa, Gaithersburg, MD). After dissociation, hippocampal neurons were resuspended in mouse nucleofector solution, transferred to an electroporation cuvette and 'nucleofected' according to the manufacturer's protocol (program O-05). For each reaction, 4×10^6 hippocampal neurons and 3 μ g siRNA were used. Neurons were then plated at a density of 20,000 cells/cm². Results obtained by nucleofection did not differ from those obtained when neurons were transfected using TransMessenger transfection reagent.

Transfection efficiency was determined by using fluorescein-labeled siRNA. For these experiments, siRNA corresponding to Ror1 or Ror2 was labeled using the Label IT[®] siRNA Tracker[™] Fluorescein Kit (Mirus, Madison, WI) according to the manufacturer's instructions. 12 hours after transfection with 100 nM fluorescein-labeled siRNA, hippocampal cultures were fixed and stained with a tubulin antibody, as described below. Control and siRNA-transfected hippocampal neurons were analyzed by fluorescence microscopy. In any given field of view, the percentage of neurons containing cytoplasmic accumulation of fluorescein was determined. At least ten fields from each of four independent experiments were analyzed.

Cell viability

Cell viability was assayed using LIVE/DEAD[®] Viability/Cytotoxicity Kit (Molecular Probes, Eugene, OR) as suggested by the manufacturer. Briefly, 2 days after plating, control, antisense- and siRNA-treated hippocampal neurons were incubated with a Calcein AM and ethidium homodimer solution for 20 minutes at 37°C. Cultures were then rinsed in PBS and viewed immediately on a Nikon fluorescent microscope.

Plasmid transfections

Expression plasmids encoding mouse Ror1 or Ror2 tagged with a Flag epitope (pcDNA3-mRor1-Flag and pcDNA3-mRor2-Flag, a generous gift from Y. Minami, Kobe University, Japan) were transfected into HEK293 cells using Lipofectamine[™] reagent (Invitrogen) as suggested by the manufacturer with some modifications. Briefly, HEK cells were plated 24 hours prior to the experiments onto poly-L-lysine-coated (100 µg/ml) coverslips in 35-mm tissue culture dishes (200,000 cells/dish). For biochemical experiments, cells were plated at high density (400,000 cells/dish). For each transfection, 5 µg of plasmid DNA was combined with 5 µl Lipofectamine[™] in 50 µl MEM and incubated in the dark for 30 minutes at room temperature to allow DNA-liposome complexes to form. Meanwhile, HEK cells were changed to serum-free MEM. The mixture was then added drop wise to the cultures and incubated at 37°C in 5% CO₂ and 90% humidity for 5 hours. After incubation, the cultures were changed to MEM plus 10% horse serum. Cells were harvested 48 hours after transfection for analysis (see below).

Hippocampal cultures (containing ~95% of pyramidal neurons and ~5% of astrocytes) were transfected before plating with pcDNA3- mRor1-Flag and pcDNA3-mRor2-Flag plasmids using the Nucleofector[™] apparatus (Amaxa). As controls, cultures were transfected with empty vector (pcDNA3) or with pEGFP-N1 (BD Biosciences, Palo Alto, CA). For each reaction, 2.5×10⁶ hippocampal neurons and 5 µg DNA were resuspended in 100 µl mouse nucleofector solution and electroporated using program O-05. Neurons were then plated at a density of 30,000 cells/cm². Two hours after transfection, the medium was changed to glia-conditioned MEM containing N2 supplements (Bottenstein and Sato, 1979) plus ovalbumin (0.1%) and sodium pyruvate (0.1 mM). Cultures were harvested 24–48 hours later and the morphology of hippocampal neurons and astrocytes was analyzed.

Immunocytochemistry

Control, sense- and antisense-treated, siRNA- and pcDNA-transfected hippocampal cultures were fixed for 20 minutes with 4% paraformaldehyde in PBS containing 0.12 M sucrose. They were then permeabilized in 0.3% Triton X-100 in PBS for 5 minutes and rinsed twice in PBS. The coverslips were preincubated in 10% bovine serum albumin (BSA) in PBS for 1 hour at room temperature and exposed to the primary antibodies (diluted in 1% BSA in PBS) overnight at 4°C. Finally, the cultures were rinsed in PBS and incubated with secondary antibodies for 1 hour at 37°C. The same protocol was followed for the immunocytochemical analysis of control, pcDNA-mRor1-Flag and pcDNA-mRor2-Flag-transfected HEK cells. The following primary antibodies were used: anti- α -tubulin (clone DM1A, 1:200; Sigma, St Louis, MO), anti-

rabbit tubulin (1:200, Sigma), anti-Ror1 and anti-Ror2 (1:100) (Paganoni and Ferreira, 2003), anti-peptide DYKDDDK (Flag) (1:500; Chemicon, Temecula, CA), antiacetylated tubulin (clone 6-11B-1, 1:50; Sigma), anti-tyrosinated tubulin (clone TUB-1A2, 1:50; Sigma), anti-GFP (1:500; BD Biosciences). The following secondary antibodies were used: anti-mouse IgG rhodamine-conjugated (Chemicon), Alexa Fluor 488 anti-mouse and Alexa Fluor 568 anti-rabbit IgG (Molecular Probes, Eugene, OR), anti-rabbit IgG biotin-conjugated (Chemicon) and Avidin-fluorescein (Roche, Indianapolis, IN). To detect actin filaments, hippocampal neurons and HEK cells were stained using phalloidin-rhodamine (1:1000; Sigma) for 1 hour at 37°C. As a negative control, one coverslip for each experimental condition was incubated with no primary antibody.

For morphometric analysis, control, sense-, antisense- and siRNA-treated hippocampal cultures that had been incubated with a tubulin antibody were exposed to biotin-conjugated rabbit anti-mouse IgG (Sigma) and then to peroxidase-conjugated mouse ExtrAvidin (Sigma) (1 hour at room temperature for each incubation). Finally, the coverslips were reacted with a substrate solution containing 0.05% 3,3'-diaminobenzidine tetrahydrochloride, 0.075% hydrogen peroxide (v/v) in 50 mM Tris-HCl, pH 7.6. Coverslips were then rinsed in deionized water to stop the developing reaction, dehydrated with graded ethanols, and finally mounted on glass slides with Permount.

Quantitative immunofluorescence analysis

Ror1, Ror2 and tubulin expression levels in hippocampal cultures were quantified densitometrically. Two-day in vitro control and siRNA-treated neurons were fixed and double stained using tubulin and Ror1 and Ror2 antibodies as described above. Background was determined by incubating one coverslip for each experimental condition with no primary antibody. Fluorescent images of equal exposure were acquired with a Photometric Cool Snap FX color digital camera on a Nikon microscope. At least 60 randomly selected hippocampal neurons per experimental condition were analyzed. Average pixel intensity after background subtraction was calculated using Metamorph Image Analysis Software (Fryer Company, Huntley, IL).

Morphometric analysis

For morphometric analysis, control, sense- and antisense-treated, and siRNA-transfected hippocampal neurons were fixed 1 or 2 days after plating and stained with a tubulin antibody as described above. Tubulin immunoreactive processes from randomly selected cells were viewed from a Nikon microscope by phase-contrast microscopy using a digital camera and traced on the screen. Plasmid-transfected hippocampal cultures were double-labeled with GFP or Flag and anti-rabbit tubulin antibodies and viewed on a Nikon fluorescent microscope. Neuritic length was determined using Metamorph Image Analysis Software. For the detection of axonal growth cones, 2 days in culture control, sense-, antisense- and siRNA-treated neurons were stained with phalloidin as described above. A growth cone was considered to be present if accumulation of actin filaments was found at the tip of the axon. Sixty to one hundred and twenty hippocampal neurons from three independent experiments were analyzed for each condition.

To determine the percentage of neurons in each developmental stage (stages I to III), control, antisense-treated, and siRNA-transfected hippocampal neurons were immunostained using a tubulin antibody and viewed on a Nikon fluorescent microscope. The number of neurons in each developmental stage was expressed as a percentage of the total number of cells in each field. 40 fields from three independent experiments were analyzed for each experimental condition. To compare the difference in developmental stages between pEGFP-N1, pcDNA3, pcDNA3-mRor1-Flag and pcDNA3-mRor2-Flag-transfected neurons, the number of

transfected neurons in each developmental stage was expressed as a percentage of the total number of transfected cells analyzed on each coverslip. For each construct, a total of 20 neurons were evaluated. Data were presented as mean \pm s.e.m. All data measurements were obtained blind as to treatment condition and subsequently analyzed using one-way ANOVA followed by Fisher's LSD post-hoc test.

Protein electrophoresis and immunoblotting

Hippocampal neurons and HEK cells were rinsed twice in warmed PBS, scraped into Laemmli buffer, and homogenized in a boiling water bath for 10 minutes. Sodium dodecyl sulfate (SDS)-polyacrylamide gels were run according to Laemmli (1970). Transfer of protein to Immobilon membranes (Millipore, Bedford, MA) and immunodetection were performed as described (Towbin et al., 1979; Ferreira et al., 1989). The following antibodies were used: anti- α -tubulin (clone DM1A, 1:100,000; Sigma); anti-Ror1 (1:500) (Paganoni and Ferreira, 2003); anti-Ror2 (1:250) (Paganoni and Ferreira, 2003); anti-MAP1B (1:1000; Endogen, Woburn, MA); anti-MAP2 (1:100; clone AP18; Sigma); anti-tau (1:1000, clone 5E2; Upstate, Lake Placid, NY and 1:10,000, clone TAU-5; Biosource); anti-peptide DYKDDDK (Flag) (1:1000; Chemicon). Secondary antibodies conjugated to HRP (1:1000; Promega, Madison, WI) followed by enhanced chemiluminescence reagents (Amersham Pharmacia Biotech, Chicago, IL) were used for the detection of proteins. In some experiments, blots were stripped in 60 mM Tris, 2% SDS and 0.8% β -mercaptoethanol at 55°C for 30 minutes and then reprobed with a different antibody. Densitometry was performed using a UMAX Power Look flatbed scanner and Adobe® PhotoShop® software on an Apple Power Mac G4 system. Films were scanned at 600 dpi using light transmittance and volume analysis was performed on the appropriate bands. Some membranes were imaged on ChemiDoc gel documentation system (BioRad, Hercules, CA). Bands were analyzed using Quantity One Analysis Software (BioRad). Results were expressed as mean \pm s.e.m. obtained from three independent experiments. Data were analyzed using one-way ANOVA followed by Fisher's LSD post-hoc test.

Reverse transcription-polymerase chain reaction (RT-PCR)

To obtain total mRNA, control, pcDNA-mRor1-Flag and pcDNA-mRor2-Flag-transfected HEK cells were lysed in TRIzol® Reagent (Life Technologies, Gaithersburg, MD) 48 hours after transfection. RNA was extracted by phenol/chloroform according to the TRIzol® Reagent manufacturer's protocol. Reverse transcription was performed in 20 μ l reactions containing 1 μ g sample RNA, 2.5 U MuLV reverse transcriptase, 2.5 μ M random hexamers, 1 U RNase inhibitor, 1 mM dATP, 1 mM dCTP, 1 mM dTTP, 1 mM dGTP, 5 mM MgCl₂ solution, 2 μ l 10 \times Buffer II (Perkin Elmer GeneAmp RNA PCR Core Kit, N808-0143). Tubes were incubated at 42°C for 15 minutes and then at 99°C for 5 minutes to terminate the reaction. To control for DNA contamination, reverse transcription was also performed in parallel tubes where MuLV reverse transcriptase was omitted. The reaction products were then subject to PCR amplification. No DNA contamination was ever detected in our samples (data not shown). PCR was performed in 82 μ l reactions (80 μ l for β -actin amplification) containing 3 μ l RT product (1 μ l for β -actin amplification), 0.2 μ M primer forward (F), 0.2 μ M primer reverse (R), 56.5 μ l deionised water, 0.25 mM dATP, 0.25 mM dCTP, 0.25 mM dTTP, 0.25 mM dGTP, 2 mM MgCl₂ solution, 8 μ l 10 \times Buffer II, 2.5 U AmpliTaq® DNA polymerase (Perkin Elmer GeneAmp RNA PCR Core Kit, N808-0143). The following primer sets were used: β -actin F (5'-GCA CCA CAC CTT CTA CAA TGA G-3'), β -actin R (5' CTC CTG AGC GCA AGT ACT CTG T-3'), corresponding to nucleotides 338-359 and 1075-1096 of the β -actin mouse sequence, respectively; Ror1 F (5'-GAG CTG CCT CTT TC- 3'), Ror1 R (5'-AGA GGC TTC CTG TTG AAA-3'), corresponding to nucleotides 1399-1412 and 1558-1575 of the Ror1 mouse sequence, respectively; Ror2 F (5'-GAG ATC AGC TTG TCC AC- 3'), Ror2 R (5'-AGC ATC GCC TCT TGC CGG-3'), corresponding to nucleotides 1399-1415 and 1563-1580 of the Ror2 mouse sequence, respectively. For the β -actin primer set, 30 cycles (0.5 minute at

95°C, 1 minute at 58°C and 1 minute at 72°C) followed by a final extension time of 7 minutes at 72°C were performed in a thermal cycler (GeneAmp[®] PCR System 2400, Perkin Elmer). For the Ror1 and Ror2 primer sets, 30 cycles (1.5 minutes at 95°C, 2 minutes at 58°C and 2 minutes at 72°C) followed by a final extension time of 7 minutes at 72°C were performed. PCR products were separated by electrophoresis on 1% agarose gels (β -actin) or 2% agarose gels (Ror1 and Ror2) and visualized by ethidium bromide staining.

Results

Suppression of Ror1 and Ror2 expression by means of antisense oligonucleotides and siRNAs

To investigate the role of Ror1 and Ror2 in neurite elongation and branching, we suppressed their expression by culturing hippocampal neurons in the presence of antisense oligonucleotides or small interfering RNA duplexes (siRNAs).

In the first set of experiments, hippocampal neurons kept in culture for 2 hours were incubated in the presence of Ror1 or Ror2 sense or antisense oligonucleotides and the expression of these RTKs was analyzed 1 and 2 days later. As described previously, Ror proteins were readily detected in the soma, neurites and growth cones of all untreated hippocampal neurons 1 and 2 days after plating (Paganoni and Ferreira, 2003) (see also Fig. 1). No changes in the expression of either Ror protein were detected in sense-treated hippocampal neurons (data not shown). On the other hand, the expression of Ror1 and Ror2 was markedly reduced in Ror1 and Ror2 antisense-treated hippocampal neurons, respectively. No Ror immunoreactivity was detected in growth cones or along the neurites extended by the majority of the Ror1 or Ror2 antisense oligonucleotide-treated neurons (~60%), whereas only faint Ror immunoreactivity was detected in the soma of these cells (Fig. 1).

To rule out potential non-specific effects of the treatment with antisense oligonucleotides, we performed the next set of experiments using RNA interference technology. This strategy has been only recently implemented for specific gene silencing in cultured primary mammalian neurons (Krichevsky and Kosik, 2002). For these experiments, hippocampal cultures were transfected with 21-mer siRNAs 2 hours after plating. These duplexes were targeted to regions of the mouse Ror1 and Ror2 sequences that did not overlap with the regions used for the antisense experiments (see Materials and Methods). We first analyzed the siRNA transfection efficiency using fluorescein-labeled siRNAs. Fluorescent siRNA spots were readily detectable in the perinuclear region of at least 30% of the hippocampal neurons present in transfected cultures (data not shown). Next, we studied the silencing effect of the Ror1 and Ror2 siRNA duplexes by immunofluorescence and western blot analysis. Ror1 and Ror2 immunoreactivities were significantly reduced in ~30% of the hippocampal neurons as compared to untreated or negative controls (Fig. 2). Negative controls included neurons transfected with scrambled oligomers (siRNA SCR), oligomers carrying a two-base pair mutation (siRNA MUT), or a siRNA targeted to a non-mammalian gene ('non-specific siRNA'). Quantitative immunofluorescence analysis was conducted next to determine the extent of Ror depletion in siRNA-treated hippocampal neurons. Images recorded with equal exposure times were obtained from randomly chosen siRNA-treated neurons and non-treated controls. Results presented as a distribution function showed a shift in immunoreactivity pixel intensity in Ror1 and Ror2 siRNA-treated neurons as compared to neurons incubated in the presence of siRNA MUT, siRNA SCR or non-treated neurons. This shift represents a specific reduction in Ror1 and Ror2 expression levels in Ror1 or Ror2 siRNA-treated neurons when compared to non-treated, siRNA SCR-treated and siRNA MUT-treated ones since no changes were detected in tubulin immunoreactivity (Fig. 2). To confirm these immunocytochemical results, whole-cell lysates from control and targeted 2-day in vitro cultures were analyzed by western blotting. In these neurons, Ror1 and Ror2 expression was knocked down by their cognate siRNA by 50%

and 25%, respectively (Fig. 3). In contrast, transfection with scrambled sequences had no effect on Ror protein expression levels (Fig. 3). Finally, we tested whether Ror1 siRNA induced changes in Ror2 expression and vice versa. No changes in Ror2 or Ror1 levels were detected when cultured hippocampal neurons were treated with Ror1 or Ror2 siRNAs, respectively (data not shown).

Effect of Ror1 and Ror2 suppression on neuronal morphology

To determine whether the suppression of Ror1 and Ror2 expression induced changes in the time course of neuronal development, we analyzed the morphological differentiation of control, antisense, and siRNA-treated hippocampal neurons during the first 2 days after plating. We chose hippocampal cultures as a model system because they provide a homogeneous population of neurons that extend neurites following a sequence of well-characterized morphological changes (Dotti et al., 1988; Goslin and Banker, 1991). Upon plating, hippocampal neurons are surrounded by a lamellipodial veil (stage I). Within the first 12 hours, the majority of the cells extend several undifferentiated neurites or minor processes (stage II). By 1 to 2 days in culture they become polarized, i.e. they extend one long process, the axon, which exceeds in length the one of the minor processes by at least 10 μm (stage III) (Goslin and Banker, 1991). The minor processes will differentiate into dendrites 4 days later (stage IV) (Dotti et al., 1988; Goslin and Banker, 1991). To analyze this sequence of morphological differentiation, we fixed and stained control and treated hippocampal cultures using a tubulin antibody. As previously described, the majority of non-treated hippocampal neurons had extended neurites during the first day in culture, thus entering stage II or III. By contrast, a significantly higher number of Ror1 and Ror2 antisense- and siRNA-treated cells had failed to elongate processes and remained in stage I when compared to Ror-expressing neurons (non-treated controls: $12\pm 2\%$ vs. Ror1 AS $23\pm 3\%*$; Ror2 AS: $38\pm 2\%*$; siRNA Ror1: $25\pm 2\%*$; siRNA Ror2: $26\pm 3\%*$. $*P<0.01$, significant difference from cell numbers in non-treated control; $n=40$ fields).

The depletion of Ror expression by means of either antisense oligonucleotides or siRNAs also resulted in morphological changes in differentiated hippocampal neurons. Stage II and stage III Ror1- and Ror2-depleted neurons were able to extend the same number of primary processes as controls (data not shown). However, Ror downregulation affected neuritic elongation. When Ror expression was targeted, neurons extended shorter minor processes than controls (Tables 1, 2; Fig. 4; see also supplementary material Fig. S1). However, the axons extended by Ror-depleted cells were longer than those elongated by Ror-expressing neurons (Tables 1, 2; Fig. 5; see also supplementary material Fig. S2). Finally, neuritic branching was reduced (Tables 1, 2; Figs 4, 5; see also supplementary material Figs S1, S2). As shown in Fig. 1, these morphological changes were restricted to Ror-depleted neurons, whereas Ror-expressing neurons in the targeted cultures resembled those in the control.

Remarkably, the phenotype of the neurons in which the expression of Ror1 and Ror2 had been suppressed by siRNA transfection was very similar to that detected in Ror-depleted neurons by means of antisense oligonucleotide treatment. However, the absolute values of neuritic length differed because these two methods required that neurons be plated at specific cell densities (Tables 1, 2).

Next, we performed a series of experiments to test whether simultaneous targeting of Ror1 and Ror2 resulted in an additive phenotype. When hippocampal neurons were treated with Ror1 and Ror2 antisense oligonucleotides at the same time, cells underwent morphological changes that were indistinguishable from those that accompanied targeting of only Ror1 or Ror2 (Table 3).

Experiments were also performed to assess whether the effects of Ror depletion by means of siRNAs or antisense oligonucleotides on neuronal morphology were dose-dependent. For these

experiments, hippocampal neurons were transfected with siRNA oligomers at concentrations ranging from 1 nM to 100 nM. Although the strongest effect on neurite elongation was detected in neurons treated with siRNAs at a concentration of 100 nM, transfection with siRNA duplexes proved effective at lower concentrations (Table 1). Decreasing the concentration of the antisense oligonucleotides from 50 μ M to 12.5 μ M also resulted in a reduction of the effect on neuronal morphology (Table 2).

As described above, the axons extended by Ror-depleted hippocampal neurons were longer and less branched than those in control neurons. In addition, some of these axons seemed to be devoid of growth cones. To easily detect and quantify the presence of axonal growth cones, 2-day in vitro control, sense-, antisense- and siRNA-treated hippocampal cultures were stained with phalloidin to detect filamentous actin highly enriched in growth cones. A growth cone was considered to be present if accumulation of F-actin was found at the tip of the axon. No difference in the percentage of axonal growth cones was detected when sense-, siRNA SCR- and siRNA MUT-treated neurons were compared to non-treated controls (data not shown). By contrast, Ror depletion by either antisense oligonucleotides or siRNAs resulted in a decrease in the percentage of hippocampal neurons bearing axonal growth cones (non-treated controls: 72 \pm 3% vs. Ror1 AS: 60 \pm 5%*; Ror2 AS: 54 \pm 2%*; siRNA Ror1: 66 \pm 1%*; siRNA Ror2: 64 \pm 1%*. * P <0.05 compared to levels in non-treated controls; n =60 neurons).

Finally, we analyzed whether the depletion of Ror proteins affected neuronal viability. No significant changes in neuronal survival were detected in cultures in which Ror1 and Ror2 expression was suppressed when compared to non-treated controls (data not shown).

Overexpression of Ror1 and Ror2 in HEK cells, astrocytes and hippocampal neurons

The phenotype of Ror1- and Ror2-depleted hippocampal neurons is consistent with a role for Ror receptors in neurite elongation. To corroborate this hypothesis, we transfected HEK cells with plasmids encoding mouse cDNAs for Ror1 or Ror2 tagged with a Flag epitope (pcDNA3-mRor1-Flag and pcDNA3- mRor2-Flag). Forty-eight hours after transfection, Ror1 and Ror2 were readily detectable by reverse transcription-polymerase chain reaction (RT-PCR), western blotting and immunocytochemistry in the cultures that had been transfected with pcDNA3-mRor1-Flag and pcDNA3-mRor2-Flag, respectively (Fig. 6). In the transfected cells, Ror1 and Ror2 were present throughout the cell body and enriched in filopodia-like protrusions whose morphology ranged from finger-like to arborized (Fig. 6C-E). Similar filopodia-like structures were detected when primary mouse astrocytes (occasionally seen in hippocampal cultures, <5% of total cells) were transfected with pcDNA3-mRor1-Flag and pcDNA3-mRor2-Flag, but not when transfected with a control pEGFP-N1 vector (Fig. 7A-C). To characterize the nature of these protrusions, control, pcDNA3-mRor1-Flag- and pcDNA3-mRor2-Flag-transfected HEK cells were double-stained with microtubular markers (acetylated tubulin as a marker of stable microtubules and tyrosinated tubulin as a marker of unstable microtubules), or microfilament markers (phalloidin as a marker of F-actin) and an anti-Flag antibody. Colocalization of Ror and actin immunoreactivity was easily detected in these protrusions (Fig. 6I-L). However, no acetylated or tyrosinated tubulin immunoreactivity was observed in the filopodia-like processes (data not shown).

Next, we analyzed the phenotypic changes that occur in hippocampal neurons upon Ror1 and Ror2 overexpression. Twenty-four hours after transfection, most of the hippocampal neurons that had been transfected with empty vector (pcDNA3) or a control GFP plasmid had elongated an axon whereas the majority of either Ror1 or Ror2-transfected neurons had not become polarized yet (pEGFP-N1 stage III: 48 \pm 2% vs. pcDNA3 stage III: 44 \pm 4%; pcDNA3- mRor1-Flag stage III: 22 \pm 5%*; pcDNA3- mRor2-Flag stage III: 17 \pm 2%*. * P <0.01 compared to number in GFP-transfected cultures; n =20 neurons). In addition, the minor neurites extended by Ror-transfected stage II neurons were abnormally branched when compared to those

extended by pcDNA3- and GFP-transfected sister cultures (Fig. 7D,F,I,L). In these cells, localization of Ror proteins was especially prominent in filopodia-like structures along the processes and in the growth cones where it colocalized with actin filaments (Fig. 7D,F,I,L and data not shown). When Ror1 and Ror2-transfected neurons were allowed to develop in culture for 48 hours, most of the cells had differentiated an axon. However, the axons extended by Ror1- and Ror2-transfected neurons were significantly shorter than those extended by pcDNA3- and GFP-transfected cells (pEGFP-N1: $164 \pm 9 \mu\text{m}$ vs. pcDNA3: $179 \pm 12 \mu\text{m}$; pcDNA3-mRor1-Flag: $125 \pm 12 \mu\text{m}^*$; pcDNA3- mRor2-Flag: $100 \pm 8 \mu\text{m}^*$. $*P < 0.01$ compared to axon length in GFP-transfected cultures; $n=20$ neurons) (Fig. 7E,G,J,M). No statistically significant changes were detected in the pattern of axonal arborization between Ror-transfected and control neurons.

Changes in microtubule-associated protein levels accompanied Ror down- and upregulation

The morphological changes induced by Ror1 and Ror2 downregulation or overexpression in different cell types strongly suggested that these RTKs participate in neurite extension. The cytoskeletal changes underlying the elongation of axons and dendrites in hippocampal neurons have been thoroughly characterized. Experimental evidence indicates that in central neurons, neurite outgrowth depends on microtubule polymerization and stabilization, which are mediated by the tightly regulated expression of the microtubule-associated protein 1B (MAP1B), MAP2 and tau (Ferreira et al., 1989; Caceres and Kosik, 1990; Caceres et al., 1992; Avila et al., 1994; Holgado and Ferreira, 2000; Gonzalez-Billault et al., 2002). As MAPs are required for normal process extension, we sought to determine whether Ror suppression and/or overexpression might affect neurite elongation by controlling their expression levels. For these experiments, whole cell lysates prepared from 2-day in vitro control, siRNA- and pcDNA-transfected neurons were analyzed by western blotting. The depletion of Ror1 and Ror2 by their cognate siRNA duplexes resulted in a significant decrease in MAP1B and MAP2 expression as compared to non-treated and scrambled siRNA-treated cultures (Fig. 8). On the other hand, when Ror1 and Ror2 were overexpressed in cultures of hippocampal neurons, MAP1B and MAP2 levels were differentially affected. Although the levels of MAP1B were decreased in Ror-overexpressing hippocampal neurons when compared to GFP-transfected sister cultures, MAP2 levels were significantly increased (Fig. 7N). Finally, no changes were detected in the levels of tau upon Ror protein down- and up-regulation (Fig. 7N, Fig. 8).

Discussion

In this study, we applied different gene silencing and overexpressing strategies to gain an insight into the role of Ror RTKs during initial stages of neuronal terminal differentiation. Our results indicate that Ror1 and Ror2 receptor tyrosine kinases differentially modulate the growth of the minor processes and the axons of cultured hippocampal neurons. In addition, we show that changes in Ror expression are accompanied by changes in the microtubule-associated proteins MAP1B and MAP2. Collectively, our findings provide the first direct evidence supporting a novel role for Ror1 and Ror2 in the signaling networks involved in neurite elongation and branching in mammalian central neurons.

Loss- and/or gain-of-function experiments have been extensively used to study the function of numerous proteins in different cell types. Unfortunately, neurons as well as other postmitotic cells, have not been easily accessible to genetic manipulations. Over a decade ago, a new experimental approach was used to block the expression of proteins in central neurons (Caceres and Kosik, 1990). In that study, the microtubule-associated protein tau was depleted in cultured cerebellar macroneurons by adding specific antisense oligonucleotides to the media (Caceres and Kosik, 1990). Since then, this technology has been widely used to establish the role of a variety of molecules in neuronal differentiation (Caceres and Kosik, 1990; Caceres et al.,

1992; Ferreira et al., 1994; Aigner and Caroni, 1995; Ferreira et al., 2000; Gonzalez-Billault et al., 2002). However, numerous factors affect the silencing efficacy and specificity of antisense oligonucleotides (selection of the target, delivery method and cell culture conditions). Recently, RNAi has become available for gene silencing in primary neurons (Eto et al., 2002; Krichevsky and Kosik, 2002; Fink et al., 2003; Higuchi et al., 2003; Passafaro et al., 2003). In this study, we used both antisense oligonucleotides and siRNA duplexes to block the expression of Ror proteins in hippocampal neurons. To our knowledge, this is the first time that these techniques have been applied in parallel to target the same molecules in mammalian primary neurons. The results presented in this study indicate that identical morphological changes were detected in neurons in which Ror expression had been suppressed by either antisense oligonucleotides or RNAi. Our findings provide evidence that these techniques can be used interchangeably to study protein function in cultured central neurons. In addition, they indicated that the Ror1/Ror2 pseudo-null phenotype is specific and does not depend on the targeted sequence or the technique used for gene silencing.

Ror depletion by means of either antisense oligonucleotides or RNAi resulted in marked abnormalities in the well-characterized sequence of events that lead to the extension of neuritic processes in cultured hippocampal neurons. A role for Ror proteins in neurite elongation was first suggested by Ror domain analysis. Interestingly, the domain organization of the extracellular region of Ror receptors shares homology with the muscle-specific kinase MuSK and Frizzled receptors (Masiakowski and Carroll, 1992; Forrester, 2002). MuSK is required for the formation of peripheral synapses as part of the receptor complex for agrin, whereas Frizzled molecules participate in neural induction, embryonic patterning, axon differentiation and synaptogenesis by mediating the activity of Wnt proteins (Valenzuela et al., 1995; Glass et al., 1996; Burden, 2000; Hall et al., 2000; Patapoutian and Reichardt, 2000; Sanes and Lichtman, 2001; Krylova et al., 2002; Packard et al., 2002). The analysis of the intracellular region of Ror proteins also points to similarities between Ror family members and other receptors that are implicated in different aspects of neuronal differentiation. In particular, the tyrosine kinase domain of Ror1 and Ror2 shares homology not only with those of MuSK, but also with Trk receptors, which mediate neurite elongation induced by neurotrophins (Davies, 2000; Labelle and Leclerc, 2000; Huang and Reichardt, 2003). These structural features suggest that Ror1 and Ror2 may share similar ligand binding properties and/or intracellular targets with MuSK, Frizzled or Trk receptors and, possibly, participate in the same developmental events.

Another clue to Ror receptor function came from studies that indicated that Ror genes are highly expressed in the developing central nervous system. Ror expression coincides with periods of active neurite extension both in vivo and in vitro, a pattern that seems to be evolutionarily conserved (Wilson et al., 1993; Oishi et al., 1997; Oishi et al., 1999; Al-Shawi et al., 2001; McKay et al., 2001; Paganoni and Ferreira, 2003). Moreover, studies conducted in our laboratory recently showed that Ror proteins are present in the neurites of developing hippocampal neurons and are concentrated in the growth cones, the 'sensory organs' of neuronal processes (Paganoni and Ferreira, 2003).

Functional studies performed in invertebrates also suggested a role for these RTKs during early stages of neuronal development. For example, in *Caenorhabditis elegans*, mutations of the Ror family member CAM-1 resulted in the disruption of cell migration, the establishment of neuronal polarity and axonal outgrowth (Forrester et al., 1999; Koga et al., 1999). More recently, mutations of *Xenopus* Ror2 (Xror2) were shown to cause disruption of convergent extension morphogenetic movements and neural plate closure via the Wnt signaling pathway, suggesting that Ror2 may mediate the activity of some Wnt family members (Hikasa et al., 2002; Oishi et al., 2003).

The findings presented in this study also support a role for these RTKs in the morphological differentiation of mammalian central neurons. Ror depletion affected the elongation of both the minor processes and the axons of hippocampal neurons. Furthermore, our results indicated that Ror receptors differentially modulate the elongation of these different cellular compartments. Although the minor processes of Ror-depleted neurons were shorter than control ones, the axons of the same cells were longer. In addition, neurite branching was decreased. Remarkably, the down-regulation of either Ror1 or Ror2 resulted in the same phenotype, suggesting that the loss of only one of the two receptors was sufficient to abolish Ror function in hippocampal neurons. This hypothesis was further supported by data indicating that the simultaneous targeting of Ror1 and Ror2 expression by antisense oligonucleotides resulted in a pseudo-null phenotype indistinguishable from that obtained when either receptor was suppressed individually. Taken together, these data suggest that Ror1 and Ror2 might interact in hippocampal neurons by forming heterodimers, as described for other RTKs (Heldin, 1995). It must be noted, however, that studies conducted on Ror1 and Ror2 knockout mice indicated that Ror proteins may be functionally redundant. Thus, Ror2 mutant mice exhibited severe skeletal abnormalities, whereas Ror1 knockouts were similar in size and gross morphology to their wild-type counterparts, although both mutant strains died perinatally (Yoda et al., 2003). Considered collectively, these data suggest that Ror2 may have a compensatory role for Ror1 loss during skeletogenesis but not during neurite elongation. Alternatively, the chronic loss of Ror1 may activate additional compensatory mechanisms in vivo that are not elicited in hippocampal neurons after acute Ror down-regulation. Further studies will be necessary to directly address the modality of interaction between Ror family members in central neurons and in non-neuronal cell types.

The phenotypic changes that we detected in hippocampal neurons upon Ror1 and Ror2 suppression are consistent with Ror proteins mediating the activity of a 'stop' factor that signals axons to stop growing, branch and differentiate. The presence of stop factors in neural circuits is well documented (Skaper et al., 2001; Tao and Poo, 2001). One putative stop factor is agrin, an extracellular matrix protein that is required for the formation of peripheral and central synapses (Cohen et al., 1997; Ji et al., 1998; Ferreira, 1999; Bose et al., 2000; Burgess et al., 2000). Interestingly, in agrin knockout mice, motor neurons grow past their target, form very few branches and exhibit impaired presynaptic differentiation (Gautam et al., 1996). Moreover, agrin-depleted hippocampal neurons elongate longer and less branched axons than control ones, whereas the elongation of their dendritic compartment is inhibited, a phenotype that reproduces that observed in Rordepleted cells (Ferreira, 1999; Mantych and Ferreira, 2001). Likewise, Wnt family members have been recently recognized as retrograde stop factors that signal axons to branch, cease extending and differentiate presynaptic terminals in multiple neuronal populations (Hall et al., 2000; Krylova et al., 2002) (our unpublished observations). As noted above, Ror1 and Ror2 share similar structural features in their extracellular domain with both MuSK, which is part of the receptor complex for agrin, and Frizzled receptors, which bind to Wnt molecules. In addition, Ror2 has been shown to interact with Wnt and Frizzled family members indicating that it may function in a multimolecular complex that mediates the activity of Wnt (Hikasa et al., 2002; Oishi et al., 2003). It will be of interest to test whether Ror1 and Ror2 are involved in the cellular responses of mammalian primary neurons to agrin and/or Wnt molecules.

A role of these RTKs in neurite elongation and branching was also supported by the gain-of-function experiments in both non-neuronal cells and hippocampal neurons. The overexpression of Ror proteins resulted in the protrusion of filopodia-like structures in non-neuronal cells. In hippocampal neurons, Ror1 or Ror2 overexpression induced the elongation of short, branched minor processes and delayed axonal growth. This phenotype is completely opposite to that observed after Ror suppression validating further the specificity of the results obtained with the loss-of-function experiments.

Combined, the Ror1 and/or Ror2 pseudo-null phenotype and the one observed after the overexpression of these RTKs provide strong support for a novel role of these receptors during early stages of neuronal terminal differentiation. However, the molecular mechanisms underlying such a role are completely unknown. The findings presented in this study provide the first insights into those mechanisms. Here we showed that Ror1 and Ror2 suppression and/or overexpression were accompanied by changes in the levels of cytoskeletal proteins (i.e. MAP1B and MAP2). Our results suggest that these MAPs may be targets of Ror-mediated signaling. In central neurons, the temporally and spatially regulated expression of the MAPs is required for the proper development of neuronal morphology (Ferreira et al., 1989; Caceres and Kosik, 1990; Caceres et al., 1992; Holgado and Ferreira, 2000; Gonzalez-Billault et al., 2002). Although the factors that finetune MAP expression are poorly understood, multiple signaling pathways triggered by receptor tyrosine kinases are known to be involved (Coffey et al., 1997; Fukumitsu et al., 1997; San Jose et al., 1997). A growing body of evidence suggests that the suppression of MAP leads to changes in the rate of growth and/or branching of neuronal processes. For example, MAP2 seems to be required for stage I to stage II transition and the elaboration of the minor processes in cultured neurons (Caceres et al., 1992). Thus, the delayed transition between stage I and stage II cells, as well as the extension of shorter and less branched minor processes observed in the absence of Ror expression may be mediated by the decrease in MAP2 expression. Conversely, the increase in MAP2 levels observed in Ror1 and/or Ror2 transfected hippocampal neurons could be responsible for the enhanced extension and branching of minor processes. Another MAP, MAP1B, seems to be associated with the extensive cytoskeletal remodeling that underlies axonal elongation and branching (Ferreira et al., 1989; Black et al., 1994; Gonzalez-Billault, 2002). In this study, we show that MAP1B protein levels are reduced when Ror1 and Ror2 expression is downregulated. We speculate that MAP1B downregulation, as well as the lack of the translation of putative stop signals due to Ror depletion, might favor axonal elongation over axonal branching in these cells. In Ror-depleted neurons, the pool of microtubular proteins may be redistributed into the main axon thus resulting in a net promotion of axonal elongation. Interestingly, MAP1B levels are also decreased in Ror-overexpressing cultures. Under these experimental conditions, the reduction in MAP1B levels combined with an enhanced transduction of stop signals could lead to increased branching and the elongation of shorter axons in Ror-overexpressing neurons.

Alternatively, Ror receptors could induce microtubule remodeling by interacting with microtubules and microfilaments. This type of interaction is supported by recent studies showing that Ror1 and Ror2 immunoreactivity was partially retained in the detergent-extracted cytoskeleton of hippocampal neurons as well as primary astrocytes (Paganoni and Ferreira, 2003; Paganoni et al., 2004). Although the molecular nature of this association awaits further investigation, these data suggest that Ror receptors may interact either directly or indirectly with neuronal microtubules and/or actin microfilaments. Interestingly, a number of receptor kinases have been shown to bind to cytoskeletal proteins and modulate their functional properties (Kadowaki et al., 1985; Nishida et al., 1987; Carman et al., 1998).

Regardless of the mechanisms, Ror proteins seem to have an important functional role in the signaling networks involved in neurite elongation and branching in mammalian central neurons. Future studies aimed at identifying ligand(s) and/or cellular targets of Ror1 and Ror2 will further our understanding of the molecular mechanisms of action of these receptors.

Acknowledgements

We thank K. Anderson for excellent technical help. We are grateful to Y. Minami (Kobe University, Japan) for generously providing the Ror1 and Ror2 expression plasmids. This work was supported by NIH grant NS 46834 to A.F.

References

- Aigner L, Caroni P. Absence of persistent spreading, branching, and adhesion in GAP-43-depleted growth cones. *J Cell Biol* 1995;128:647–660. [PubMed: 7860637]
- Al-Shawi R, Ashton SV, Underwood C, Simons JP. Expression of the Ror1 and Ror2 receptor tyrosine kinase genes during mouse development. *Dev Genes Evol* 2001;211:161–171. [PubMed: 11455430]
- Avila J, Dominguez J, Diaz-Nido J. Regulation of microtubule dynamics by microtubule-associated protein expression and phosphorylation during neuronal development. *Int J Dev Biol* 1994;38:13–25. [PubMed: 8074993]
- Black MM, Slaughter T, Fischer I. Microtubule-associated protein 1b (MAP1b) is concentrated in the distal region of growing axons. *J Neurosci* 1994;14:857–870. [PubMed: 8301365]
- Bose CM, Qiu D, Bergamaschi A, Gravante B, Bossi M, Villa A, Rupp F, Malgaroli A. Agrin controls synaptic differentiation in hippocampal neurons. *J Neurosci* 2000;20:9086–9095. [PubMed: 11124985]
- Bottenstein JE, Sato GH. Growth of a rat neuroblastoma cell line in serum-free supplemented medium. *Proc Natl Acad Sci USA* 1979;76:514–517. [PubMed: 284369]
- Burden SJ. Wnts as retrograde signals for axon and growth cone differentiation. *Cell* 2000;100:495–497. [PubMed: 10721986]
- Burgess RW, Skarnes WC, Sanes JR. Agrin isoforms with distinct amino termini: differential expression, localization, and function. *J Cell Biol* 2000;151:41–52. [PubMed: 11018052]
- Caceres A, Kosik KS. Inhibition of neurite polarity by tau antisense oligonucleotides in primary cerebellar neurons. *Nature* 1990;343:461–463. [PubMed: 2105469]
- Caceres A, Mautino J, Kosik KS. Suppression of MAP2 in cultured cerebellar macroneurons inhibits minor neurite formation. *Neuron* 1992;9:607–618. [PubMed: 1389180]
- Carman CV, Som T, Kim CM, Benovic JL. Binding and phosphorylation of tubulin by G protein-coupled receptor kinases. *J Biol Chem* 1998;273:20308–20316. [PubMed: 9685381]
- Coffey ET, Akerman KE, Courtney MJ. Brain derived neurotrophic factor induces a rapid upregulation of synaptophysin and tau proteins via the neurotrophin receptor TrkB in rat cerebellar granule cells. *Neurosci Lett* 1997;227:177–180. [PubMed: 9185679]
- Cohen NA, Kaufmann WE, Worley PF, Rupp F. Expression of agrin in the developing and adult rat brain. *Neuroscience* 1997;76:581–596. [PubMed: 9015340]
- Craig AM, Banker GA. Neuronal polarity. *Annu Rev Neurosci* 1994;17:267–310. [PubMed: 8210176]
- Davies AM. Neurotrophins: neurotrophic modulation of neurite growth. *Curr Biol* 2000;10:R198–R200. [PubMed: 10712898]
- Dickson BJ. Molecular mechanisms of axon guidance. *Science* 2002;298:1959–1964. [PubMed: 12471249]
- Dotti CG, Sullivan CA, Banker GA. The establishment of polarity by hippocampal neurons in culture. *J Neurosci* 1988;8:1454–1468. [PubMed: 3282038]
- Elbashir SM, Harborth J, Lendeckel W, Yalcin A, Weber K, Tuschl T. Duplexes of 21-nucleotide RNAs mediate RNA interference in cultured mammalian cells. *Nature* 2001a;411:494–498. [PubMed: 11373684]
- Elbashir SM, Martinez J, Patkaniowska A, Lendeckel W, Tuschl T. Functional anatomy of siRNAs for mediating efficient RNAi in *Drosophila melanogaster* embryo lysate. *EMBO J* 2001b;20:6877–6888. [PubMed: 11726523]
- Eto M, Bock R, Brautigam DL, Linden DJ. Cerebellar long-term synaptic depression requires PKC-mediated activation of CPI-17, a myosin/oesin phosphatase inhibitor. *Neuron* 2002;36:1145–1158. [PubMed: 12495628]
- Ferreira A. Abnormal synapse formation in agrin-depleted hippocampal neurons. *J Cell Sci* 1999;112:4729–4738. [PubMed: 10574720]
- Ferreira A, Busciglio J, Caceres A. Microtubule formation and neurite growth in cerebellar macroneurons which develop in vitro: evidence for the involvement of the microtubule-associated proteins, MAP-1a, HMW-MAP2 and Tau. *Brain Res Dev Brain Res* 1989;49:215–228.

- Ferreira A, Kosik KS, Greengard P, Han HQ. Aberrant neurites and synaptic vesicle protein deficiency in synapsin II-depleted neurons. *Science* 1994;264:977–979. [PubMed: 8178158]
- Ferreira A, Kao HT, Feng J, Rapoport M, Greengard P. Synapsin III: developmental expression, subcellular localization, and role in axon formation. *J Neurosci* 2000;20:3736–3744. [PubMed: 10804215]
- Fink CC, Bayer KU, Myers JW, Ferrell JE Jr, Schulman H, Meyer T. Selective regulation of neurite extension and synapse formation by the beta but not the alpha isoform of CaMKII. *Neuron* 2003;39:283–297. [PubMed: 12873385]
- Forrester WC. The Ror receptor tyrosine kinase family. *Cell Mol Life Sci* 2002;59:83–96. [PubMed: 11846036]
- Forrester WC, Dell M, Perens E, Garriga G. A *C. elegans* Ror receptor tyrosine kinase regulates cell motility and asymmetric cell division. *Nature* 1999;400:881–885. [PubMed: 10476968]
- Fukumitsu H, Ohashi A, Nitta A, Nomoto H, Furukawa S. BDNF and NT-3 modulate expression and threonine phosphorylation of microtubule-associated protein 2 analogues, and alter their distribution in the developing rat cerebral cortex. *Neurosci Lett* 1997;238:107–110. [PubMed: 9464631]
- Gautam M, Noakes PG, Moscoso L, Rupp F, Scheller RH, Merlie JP, Sanes JR. Defective neuromuscular synaptogenesis in agrin-deficient mutant mice. *Cell* 1996;85:525–535. [PubMed: 8653788]
- Glass DJ, Bowen DC, Stitt TN, Radziejewski C, Bruno J, Ryan TE, Gies DR, Shah S, Mattsson K, Burden SJ, et al. Agrin acts via a MuSK receptor complex. *Cell* 1996;85:513–523. [PubMed: 8653787]
- Gonzalez-Billault C, Engelke M, Jimenez-Mateos EM, Wandosell F, Caceres A, Avila J. Participation of structural microtubule-associated proteins (MAPs) in the development of neuronal polarity. *J Neurosci Res* 2002;67:713–719. [PubMed: 11891784]
- Goslin, K. and Banker, G. A. (1991). Rat hippocampal neurons in low-density culture. In: *Culturing nerve cells* (ed. G. A. Banker and K. Goslin), pp. 251–283. Cambridge, MA: The MIT Press.
- Hall AC, Lucas FR, Salinas PC. Axonal remodeling and synaptic differentiation in the cerebellum is regulated by WNT-7a signaling. *Cell* 2000;100:525–535. [PubMed: 10721990]
- Heldin CH. Dimerization of cell surface receptors in signal transduction. *Cell* 1995;80:213–223. [PubMed: 7834741]
- Higuchi H, Yamashita T, Yoshikawa H, Tohyama M. Functional inhibition of the p75 receptor using a small interfering RNA. *Biochem Biophys Res Commun* 2003;301:804–809. [PubMed: 12565852]
- Hikasa H, Shibata M, Hiratani I, Taira M. The *Xenopus* receptor tyrosine kinase Xror2 modulates morphogenetic movements of the axial mesoderm and neuroectoderm via Wnt signaling. *Development* 2002;129:5227–5239. [PubMed: 12399314]
- Holgado A, Ferreira A. Synapse formation proceeds independently of dendritic elongation in cultured hippocampal neurons. *J Neurobiol* 2000;43:121–131. [PubMed: 10770841]
- Huang EJ, Reichardt LF. Trk receptors: roles in neuronal signal transduction. *Annu Rev Biochem* 2003;72:609–642. [PubMed: 12676795]
- Ji RR, Bose CM, Lesuisse C, Qiu D, Huang JC, Zhang Q, Rupp F. Specific agrin isoforms induce cAMP response element binding protein phosphorylation in hippocampal neurons. *J Neurosci* 1998;18:9695–9702. [PubMed: 9822730]
- Kadowaki T, Fujita-Yamaguchi Y, Nishida E, Takaku F, Akiyama T, Kathuria S, Akanuma Y, Kasuga M. Phosphorylation of tubulin and microtubule-associated proteins by the purified insulin receptor kinase. *J Biol Chem* 1985;260:4016–4020. [PubMed: 3920212]
- Klein R. Excitatory Eph receptors and adhesive ephrin ligands. *Curr Opin Cell Biol* 2001;13:196–203. [PubMed: 11248553]
- Koga M, Takeuchi M, Tameishi T, Ohshima Y. Control of DAF-7 TGF- α expression and neuronal process development by a receptor tyrosine kinase KIN-8 in *Caenorhabditis elegans*. *Development* 1999;126:5387–5398. [PubMed: 10556063]
- Krichevsky AM, Kosik KS. RNAi functions in cultured mammalian neurons. *Proc Natl Acad Sci USA* 2002;99:11926–11929. [PubMed: 12192088]
- Krylova O, Herreros J, Cleverley KE, Ehler E, Henriquez JP, Hughes SM, Salinas PC. WNT-3, expressed by motoneurons, regulates terminal arborization of neurotrophin-3-responsive spinal sensory neurons. *Neuron* 2002;35:1043–1056. [PubMed: 12354395]

- Labelle C, Leclerc N. Exogenous BDNF, NT-3 and NT-4 differentially regulate neurite outgrowth in cultured hippocampal neurons. *Brain Res Dev Brain Res* 2000;123:1–11.
- Laemmli UK. Cleavage of structural proteins during the assembly of the head of bacteriophage T4. *Nature* 1970;227:680–685. [PubMed: 5432063]
- Mantych KB, Ferreira A. Agrin differentially regulates the rates of axonal and dendritic elongation in cultured hippocampal neurons. *J Neurosci* 2001;21:6802–6809. [PubMed: 11517268]
- Masiakowski P, Carroll RD. A novel family of cell surface receptors with tyrosine kinase-like domain. *J Biol Chem* 1992;267:26181–26190. [PubMed: 1334494]
- McKay SE, Hislop J, Scott D, Bulloch AG, Kaczmarek LK, Carew TJ, Sossin WS. Aplysia ror forms clusters on the surface of identified neuroendocrine cells. *Mol Cell Neurosci* 2001;17:821–841. [PubMed: 11358481]
- Mueller BK. Growth cone guidance: first steps towards a deeper understanding. *Annu Rev Neurosci* 1999;22:351–388. [PubMed: 10202543]
- Nishida E, Hoshi M, Miyata Y, Sakai H, Kadowaki T, Kasuga M, Saijo S, Ogawara H, Akiyama T. Tyrosine phosphorylation by the epidermal growth factor receptor kinase induces functional alterations in microtubule-associated protein 2. *J Biol Chem* 1987;262:16200–16204. [PubMed: 2824482]
- Oishi I, Sugiyama S, Liu ZJ, Yamamura H, Nishida Y, Minami Y. A novel Drosophila receptor tyrosine kinase expressed specifically in the nervous system. Unique structural features and implication in developmental signaling. *J Biol Chem* 1997;272:11916–11923. [PubMed: 9115253]
- Oishi I, Takeuchi S, Hashimoto R, Nagabukuro A, Ueda T, Liu ZJ, Hatta T, Akira S, Matsuda Y, Yamamura H, et al. Spatiotemporally regulated expression of receptor tyrosine kinases, mRor1, mRor2, during mouse development: implications in development and function of the nervous system. *Genes Cells* 1999;4:41–56. [PubMed: 10231392]
- Oishi I, Suzuki H, Onishi N, Takada R, Kani S, Ohkawara B, Koshida I, Suzuki K, Yamada G, Schwabe GC, et al. The receptor tyrosine kinase Ror2 is involved in non-canonical Wnt5a/JNK signalling pathway. *Genes Cells* 2003;8:645–654. [PubMed: 12839624]
- Packard M, Koo ES, Gorczyca M, Sharpe J, Cumberledge S, Budnik V. The Drosophila Wnt, wingless, provides an essential signal for pre- and postsynaptic differentiation. *Cell* 2002;111:319–330. [PubMed: 12419243]
- Paganoni S, Ferreira A. Expression and subcellular localization of Ror tyrosine kinase receptors are developmentally regulated in cultured hippocampal neurons. *J Neurosci Res* 2003;73:429–440. [PubMed: 12898527]
- Paganoni S, Anderson KL, Ferreira A. Differential subcellular localization of Ror tyrosine kinase receptors in cultured astrocytes. *Glia* 2004;46:456–466. [PubMed: 15095375]
- Passafaro M, Nakagawa T, Sala C, Sheng M. Induction of dendritic spines by an extracellular domain of AMPA receptor subunit GluR2. *Nature* 2003;424:677–681. [PubMed: 12904794]
- Patapoutian A, Reichardt LF. Roles of Wnt proteins in neural development and maintenance. *Curr Opin Neurobiol* 2000;10:392–399. [PubMed: 10851180]
- San Jose I, Vazquez E, Garcia-Atares N, Huerta JJ, Vega JA, Represa J. Differential expression of microtubule associated protein MAP-2 in developing cochleovestibular neurons and its modulation by neurotrophin-3. *Int J Dev Biol* 1997;41:509–519. [PubMed: 9240568]
- Sanes JR, Lichtman JW. Induction, assembly, maturation and maintenance of a postsynaptic apparatus. *Nat Rev Neurosci* 2001;2:791–805. [PubMed: 11715056]
- Schlessinger J. Cell signaling by receptor tyrosine kinases. *Cell* 2000;103:211–225. [PubMed: 11057895]
- Skaper SD, Moore SE, Walsh FS. Cell signalling cascades regulating neuronal growth-promoting and inhibitory cues. *Prog Neurobiol* 2001;65:593–608. [PubMed: 11728645]
- Tanaka E, Sabry J. Making the connection: cytoskeletal rearrangements during growth cone guidance. *Cell* 1995;83:171–176. [PubMed: 7585934]
- Tao HW, Poo M. Retrograde signaling at central synapses. *Proc Natl Acad Sci USA* 2001;98:11009–11015. [PubMed: 11572961]
- Towbin H, Staehelin T, Gordon J. Electrophoretic transfer of proteins from polyacrylamide gels to nitrocellulose sheets: procedure and some applications. *Proc Natl Acad Sci USA* 1979;76:4350–4354. [PubMed: 388439]

- Valenzuela DM, Stitt TN, DiStefano PS, Rojas E, Mattsson K, Compton DL, Nunez L, Park JS, Stark JL, Gies DR, et al. Receptor tyrosine kinase specific for the skeletal muscle lineage: expression in embryonic muscle, at the neuromuscular junction, and after injury. *Neuron* 1995;15:573–584. [PubMed: 7546737]
- Wilson C, Goberdhan DC, Steller H. Dror, a potential neurotrophic receptor gene, encodes a Drosophila homolog of the vertebrate Ror family of Trk-related receptor tyrosine kinases. *Proc Natl Acad Sci USA* 1993;71:9–7113. [PubMed: 8394009]
- Yoda A, Oishi I, Minami Y. Expression and function of the Ror-family receptor tyrosine kinases during development: lessons from genetic analyses of nematodes, mice, and humans. *J Recept Signal Transduct Res* 2003;23:1–15. [PubMed: 12680586]

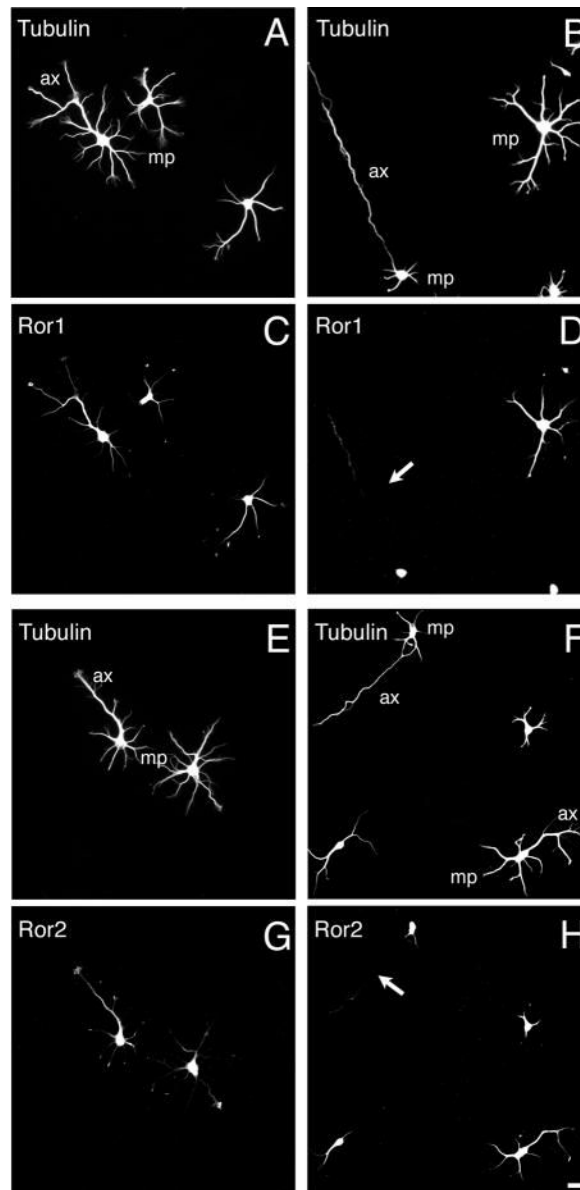


Fig. 1. Ror1 and Ror2 suppression by antisense oligonucleotide treatment in cultured hippocampal neurons. 2-day cultured control (A,C,E,G), Ror1 antisense- (B,D) and Ror2 antisense- (F,H) treated hippocampal neurons were double stained with tubulin (A,B,E,F) and Ror1 (C,D) or Ror2 (G,H) antibodies. Ror1 and Ror2 were readily detectable in the soma, the neurites and the growth cones of control neurons (C,G). On the other hand, very little Ror immunoreactivity was found in many of the neurons treated with Ror1 or Ror2 oligonucleotides (arrows in D,H). Tubulin expression was not affected by Ror1 and Ror2 antisense oligonucleotide treatment (B,F). ax, axon; mp, minor process. Bar, 20 μ m.

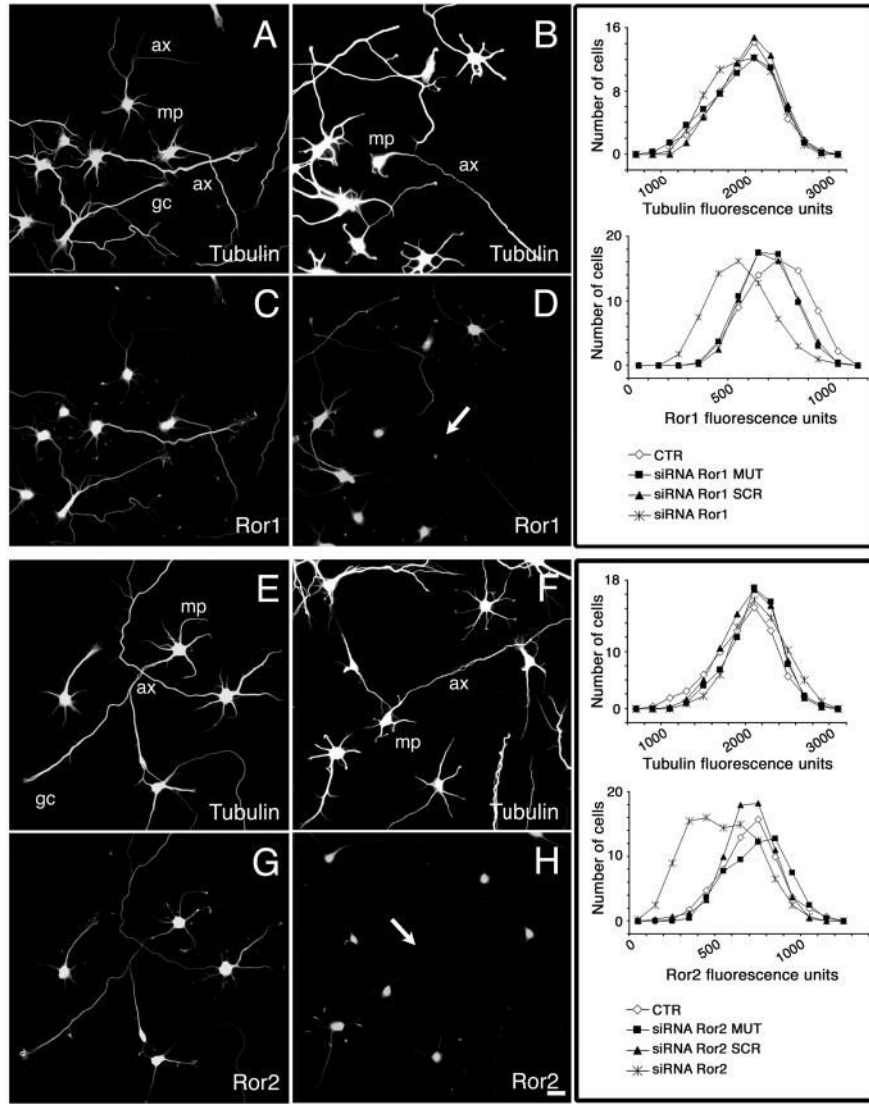


Fig. 2. Ror1 and Ror2 suppression by RNAi in cultured hippocampal neurons. (A-H) 2- day cultured control (A,C,E,G), siRNA Ror1- (B,D) and siRNA Ror2- (F,H) treated hippocampal neurons were double stained with tubulin (A,B,E,F) and Ror1 (C,D) or Ror2 (G,H) antibodies. Transfection with the cognate siRNA duplex reduced Ror1 and Ror2 expression in neurons from the targeted cultures (arrows in D,H), leaving their tubulin expression unaffected (B,F). Panels on the right represent the distribution function of the immunoreactivity pixel intensity of the immunoreactivity of Ror1 and tubulin (upper panel) and Ror2 and tubulin (lower panel) in control and targeted hippocampal neurons. Controls included non-transfected neurons (CTR) and neurons transfected with oligomers carrying a 2 base pair mutation (siRNA MUT) or scrambled oligomers (siRNA SCR). Note the shift in the expression levels of Ror1 and Ror2, but not of tubulin, in the targeted cultures when compared to controls. ax, axon; gc, growth cone; mp, minor process. Bar, 20 μ m.

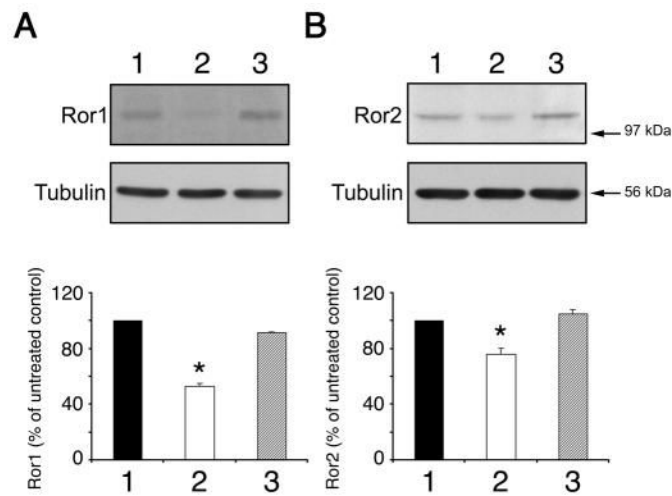


Fig. 3.

Reduction of Ror1 and Ror2 expression by RNAi in hippocampal cultures. Western blot analysis of whole cell extracts prepared from 2-day in vitro untreated hippocampal cultures (A and B, lane 1), cultures that had been transfected with Ror1 (A, lane 2) or Ror2 (B, lane 2) siRNA duplexes and cultures that had been transfected with the corresponding scrambled oligomers (A and B, lane 3). The proteins were separated by SDS-PAGE and immunoblots were reacted with Ror1 (A) and Ror2 (B) antibodies. Densitometries of the immunoreactive bands are shown under the blot. Values were normalized using tubulin as an internal control. The results correspond to the percentage of Ror1 and Ror2 protein present in the RNAi-transfected cultures as compared to the levels detected in the untreated controls (100%). * $P < 0.01$ compared to levels in untreated and scrambled siRNA-treated cultures.

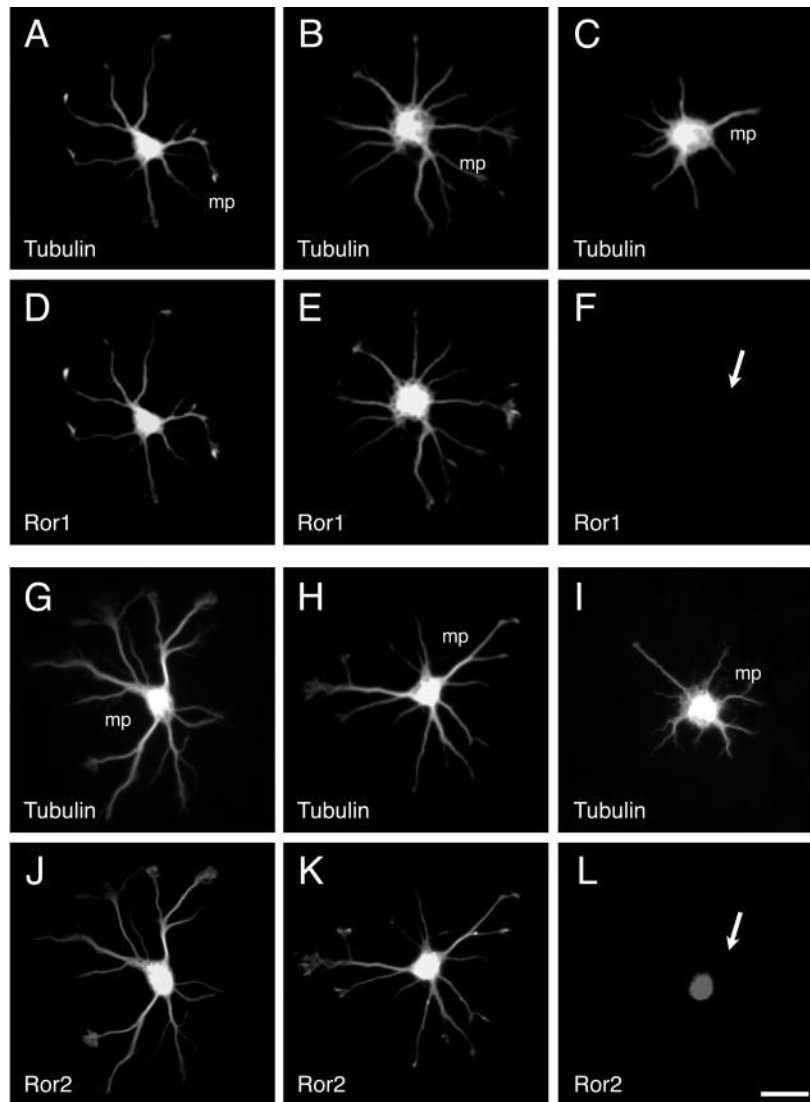


Fig. 4. Effect of Ror1 and Ror2 suppression by antisense oligonucleotide treatment on stage II hippocampal neurons. One-day cultured control (A,D,G,J), Ror1 sense-treated (B,E), Ror2 sense-treated (H,K), Ror1 antisense-treated (C,F) and Ror2 antisense-treated (I,L) hippocampal neurons were double stained with tubulin (A-C, G-I) and Ror1 (D-F) or Ror2 (J-L) antibodies. Ror1 and Ror2 suppression by the corresponding antisense oligonucleotide (arrows in F,L) was accompanied by the elongation of shorter and less branched minor processes (mp). Bar, 20 μ m.

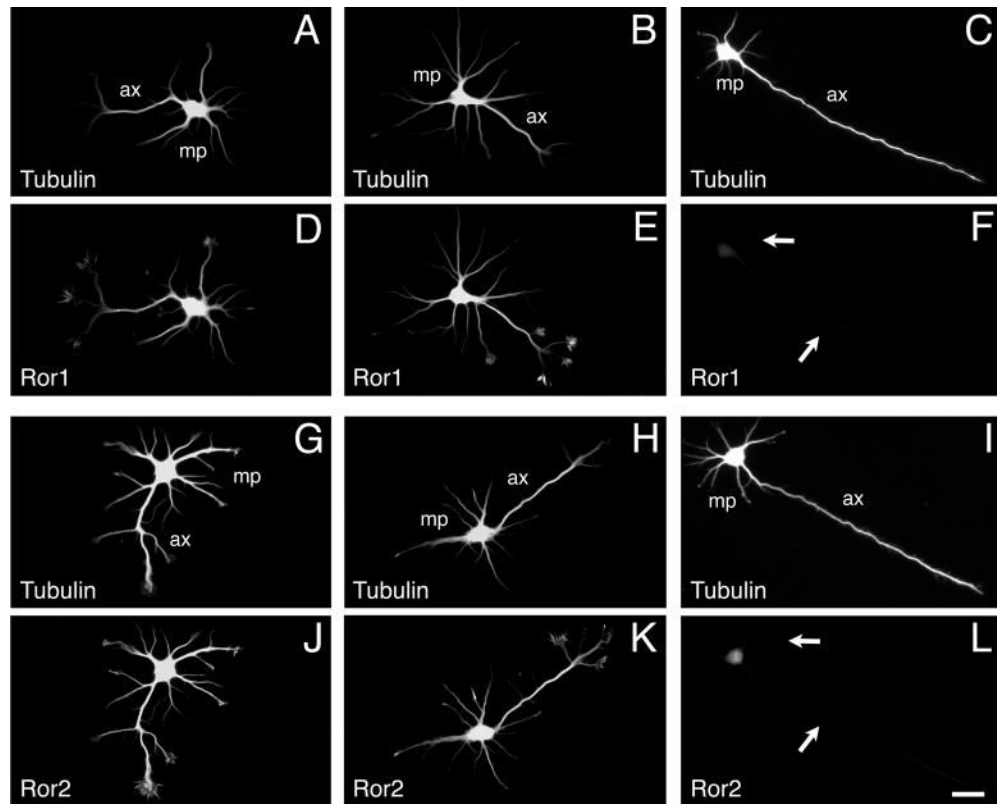


Fig. 5. Effect of Ror1 and Ror2 suppression by antisense oligonucleotide treatment on stage III hippocampal neurons. 2-day in culture control (A,D,G,J), Ror1 sense-treated (B,E), Ror2 sense-treated (H,K), Ror1 antisense-treated (C,F) and Ror2 antisense-treated (I,L) hippocampal neurons were double stained with tubulin (A-C, G-I) and Ror1 (D-F) or Ror2 (J-L) antibodies. Ror-depleted neurons elongated shorter minor processes (mp) but longer axons (ax) than control neurons (arrows in F,L). Bar, 20 μ m.

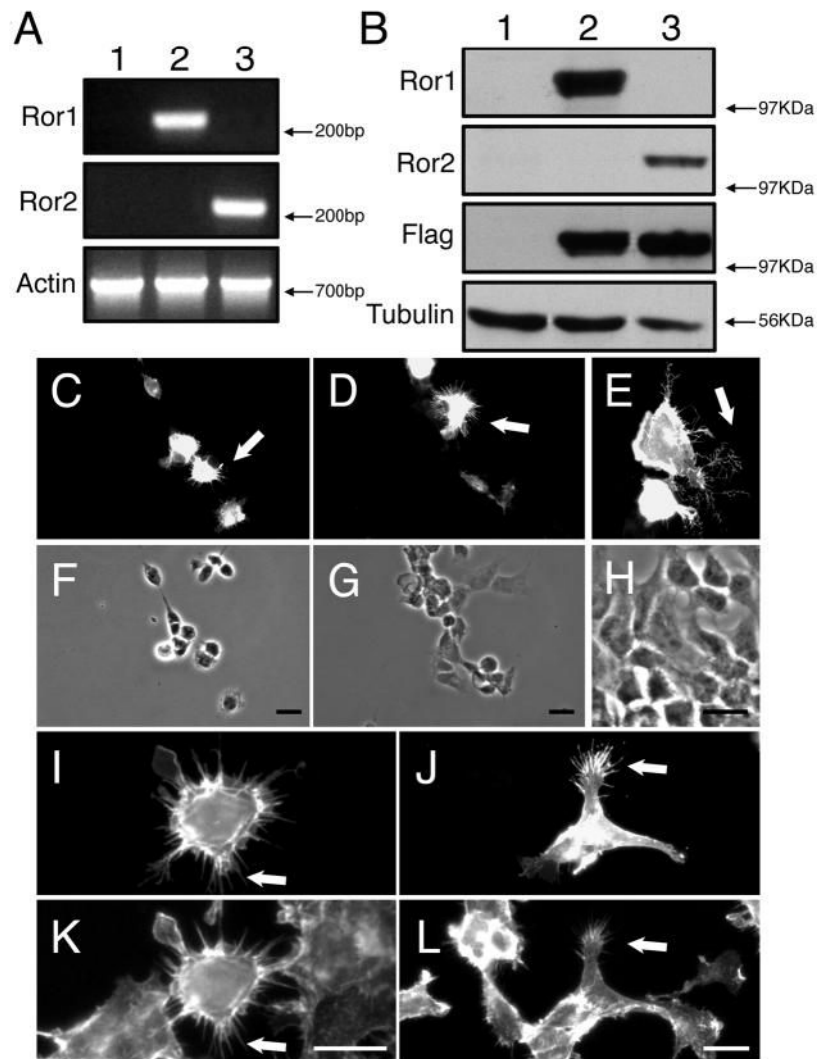


Fig. 6. Overexpression of Ror1 and Ror2 in HEK cells. HEK cells were transfected with expression plasmids encoding mouse Ror1 or Ror2 cDNAs and harvested 48 hours later for analysis. (A) Reverse transcription-polymerase chain reaction (RT-PCR) and (B) western blot analysis of pcDNA3-mRor1-Flag (A and B, lane 2) and pcDNA3-mRor2-Flag (A and B, lane 3) transfected HEK cultures. As a control, untreated HEK cultures were used (A and B, lane 1). (C-H) pcDNA3-mRor1-Flag-transfected (C,E,F,H) and pcDNA3-mRor2-Flag-transfected (D,G) HEK cells were stained with anti-Flag (C,D) or anti-Ror1 (E) antibodies. Note the distribution of Ror1 and Ror2 in the soma and in filopodia-like protrusions (arrows in C-E). (I-L) pcDNA3-mRor1-Flag-transfected (I,K) and pcDNA3-mRor2-Flag-transfected (J,L) HEK cells were stained with an anti-Flag antibody (I,J) and counterstained with phalloidin (K,L) to demonstrate the colocalization of Ror proteins with F-actin (arrows in I-L). Bar, 20 μ m.

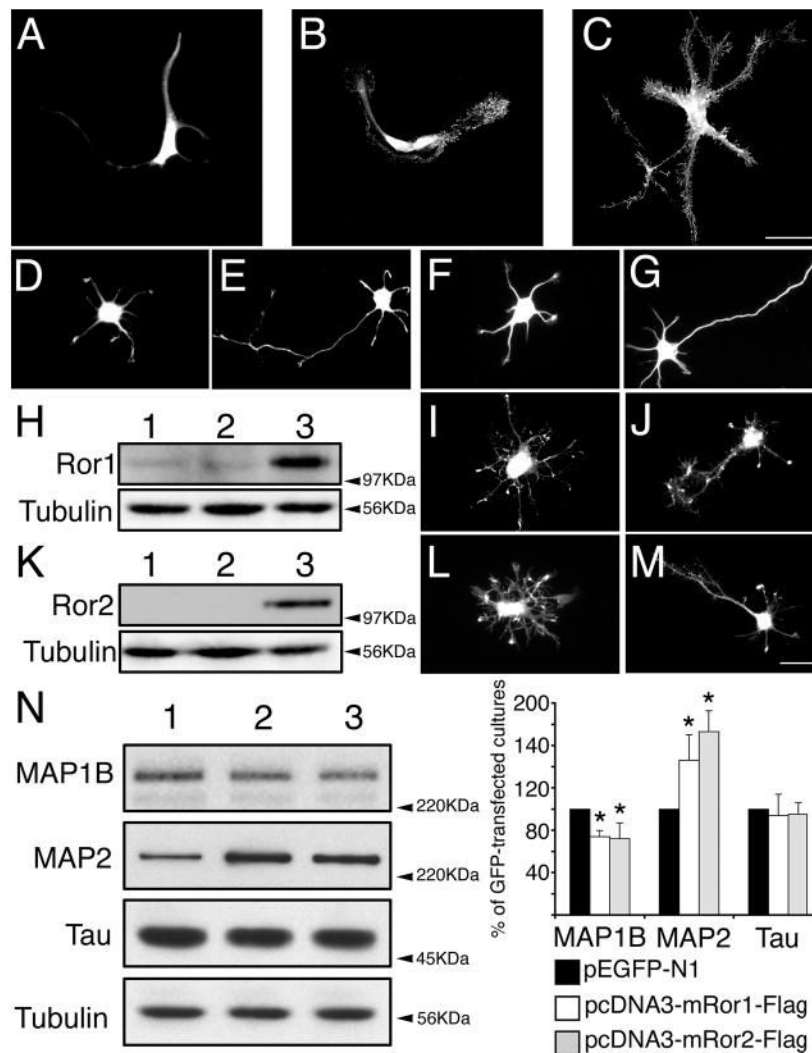


Fig. 7. Overexpression of Ror1 and Ror2 in astrocytes and hippocampal neurons. Primary astrocytes (A-C) and hippocampal neurons (D-M) were transfected with pEGFP-N1 (A,D,E), pcDNA3 (F,G), pcDNA3-mRor1-Flag (B,I,J) or pcDNA3- mRor2-Flag (C,L,M). Cultures were fixed 24 (A-D, F,I,L) or 48 (E,G,J,M) hours later and stained with GFP (A,D,E), tubulin (F,G) or Flag (B,C,I,J,L,M) antibodies. (H) Lysates from 2-day in vitro sister cultures were analyzed by western blotting to demonstrate overexpression of Ror1. pcDNA3, pEGFP-N1- and pcDNA3-mRor1- Flag-transfected cultures were loaded in lanes 1, 2 and 3, respectively. Membranes were probed with anti-Ror1 and tubulin antibodies. A tenfold increase in Ror1 expression was detected, compared to control levels. (K) Lysates from 2-day in vitro sister cultures of hippocampal neurons were analyzed by western blotting to demonstrate overexpression of Ror2. pcDNA3, pEGFP-N1- and pcDNA3-mRor2- Flag-transfected cultures were loaded in lanes 1, 2 and 3, respectively. Membranes were probed with anti-Flag and tubulin antibodies. (N) Lysates from 2-day in vitro sister cultures were subjected to western blot analysis (pEGFP-N1-, pcDNA3- mRor1-Flag- and pcDNA3-mRor2-Flag-transfected cultures were loaded in lanes 1, 2 and 3, respectively). Densitometries of the immunoreactive bands obtained by western blotting with MAP1B, MAP2 and tau antibodies are shown. The results correspond to the percentage of MAP1B, MAP2 and tau protein levels present in the

pcDNA3-mRor1- and pcDNA3-mRor2-Flag-transfected cultures when considering the levels in the GFP-transfected samples as 100%. * $P < 0.01$ compared to protein levels in pEGFP-N1-transfected cultures. Bar, 20 μm .

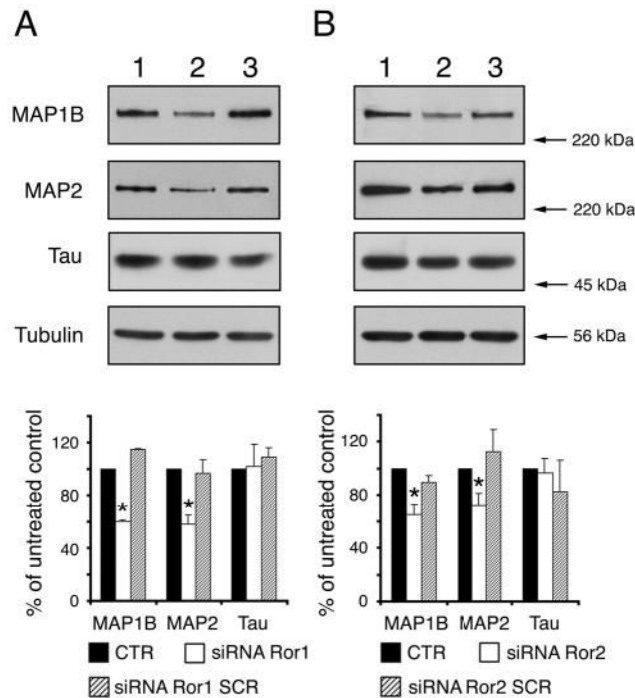


Fig. 8.

Ror suppression is accompanied by changes in the levels of the microtubule-associated proteins MAP1B and MAP2. Western blot analysis of whole cell extracts prepared from 2-day in vitro untreated hippocampal cultures (A and B, lane 1), cultures that had been transfected with Ror1 (A, lane 2) or Ror2 (B, lane 2) siRNA duplexes and cultures that had been transfected with the corresponding scrambled siRNAs (A and B, lane 3). Densitometries of the immunoreactive bands obtained by western blotting with MAP1B, MAP2 and tau antibodies are shown below the blots. The results correspond to the percent of MAP1B, MAP2 and tau protein levels present in the siRNA-transfected cultures when considering the levels in the control samples as 100%. Note the significant decrease of MAP1B and MAP2, but not tau, levels in the siRNA Ror1 and Ror2-treated cultures when compared to levels in control cells. * $P < 0.01$ when compared to levels in untreated and scrambled siRNA-treated cultures.

Table 1
Effect of Ror1 and Ror2 suppression by RNAi on neurite elongation in hippocampal neurons

Days in culture	Treatment siRNA duplex	Dose (nM)	Primary minor process length (μm)	% Branched primary minor processes	Primary axon length (μm)	Number of branches/axon
1	None	—	37 \pm 1	45 \pm 3	—	—
1	Non-specific siRNA	100	37 \pm 2	38 \pm 3	—	—
1	siRNA Ror1 SCR	100	35 \pm 0	47 \pm 2	—	—
1	siRNA Ror1 MUT	100	37 \pm 1	47 \pm 4	—	—
1	siRNA Ror2 SCR	100	35 \pm 0	44 \pm 3	—	—
1	siRNA Ror2 MUT	100	34 \pm 1	43 \pm 4	—	—
1	siRNA Ror1	100	28 \pm 1*	26 \pm 2*	—	—
1	siRNA Ror2	100	30 \pm 1*	32 \pm 2*	—	—
2	None	—	46 \pm 2	44 \pm 3	190 \pm 6	2.2 \pm 0.1
2	Non-specific siRNA	100	43 \pm 2	37 \pm 3	181 \pm 7	1.7 \pm 0.1
2	siRNA Ror1 SCR	100	41 \pm 2	51 \pm 4	164 \pm 5	2.7 \pm 0.2
2	siRNA Ror1 MUT	100	40 \pm 2	44 \pm 3	192 \pm 8	2.2 \pm 0.1
2	siRNA Ror2 SCR	100	41 \pm 2	58 \pm 5	165 \pm 5	2.3 \pm 0.2
2	siRNA Ror2 MUT	100	39 \pm 2*	44 \pm 3	186 \pm 6	1.8 \pm 0.1*
2	siRNA Ror1	100	35 \pm 2*	25 \pm 2*	241 \pm 8*	1.4 \pm 0.1*
2	siRNA Ror2	50	33 \pm 2*	34 \pm 4	222 \pm 10*	1.4 \pm 0.1*
2	siRNA Ror1	10	33 \pm 3	35 \pm 4	226 \pm 10*	1.4 \pm 0.1*
2	siRNA Ror2	1	38 \pm 2	41 \pm 4	192 \pm 9	2.1 \pm 0.2*
2	siRNA Ror1	100	33 \pm 2*	28 \pm 3*	210 \pm 6*	1.5 \pm 0.1*
2	siRNA Ror2	50	32 \pm 2*	34 \pm 3	207 \pm 8	1.4 \pm 0.1*
2	siRNA Ror1	10	34 \pm 2*	36 \pm 4	209 \pm 10	1.3 \pm 0.1*
2	siRNA Ror2	1	34 \pm 2*	35 \pm 4	201 \pm 8	1.6 \pm 0.1

E16 hippocampal cultures were plated at 250,000 cells/dish and allowed to develop for 1 (stage II) or 2 (stage III) days. Cells were fixed and stained with a tubulin antibody (clone DM1A). Neuritic processes from randomly selected cells were viewed by phase microscopy using a digital camera and traced on the screen. Neuritic length was determined using Metamorph Image Analysis Software. At least 90 cells from three independent experiments were analyzed for each condition. Results are expressed as mean \pm s.e.m.

* $P < 0.01$ compared to measurements in all controls.

Non-specific siRNA, siRNA targeted against a non-mammalian gene; siRNA SCR, siRNA containing a scrambled sequence; siRNA MUT, siRNA containing a 2 base pair change.

Table 2
Effect of Ror1 and Ror2 suppression by means of antisense oligonucleotides on neurite elongation in hippocampal neurons

Days in culture	Treatment (oligonucleotide)	Dose (μ M)	Primary minor process length (μ m)	% Branched primary processes	Primary axon length (μ m)	Number of branches/axon
1	None	—	35 \pm 3	35 \pm 4	—	—
1	Sense Ror1 (+80+97)	50	33 \pm 7	34 \pm 2	—	—
1	Sense Ror2 (+24+41)	50	32 \pm 7	35 \pm 2	—	—
1	Antisense Ror1 (+80+97)	50	25 \pm 9 ^{*†}	15 \pm 3 ^{*†}	—	—
1	Antisense Ror2 (+24+41)	50	26 \pm 8 ^{*†}	14 \pm 3 ^{*†}	—	—
2	None	—	41 \pm 2	60 \pm 1	100 \pm 3	3.3 \pm 0.3
2	Sense Ror1 (+80+97)	50	34 \pm 2	64 \pm 1	103 \pm 7	2.1 \pm 0.2
2	Sense Ror2 (+24+41)	50	38 \pm 2	60 \pm 1 ^{*†}	109 \pm 7	2.3 \pm 0.2
2	Antisense Ror1 (+80+97)	50	28 \pm 2 ^{*†}	30 \pm 1 ^{*†}	155 \pm 9 ^{*†}	1.7 \pm 0.2 [*]
2	Antisense Ror1 (+80+97)	25	29 \pm 2 ^{*†}	30 \pm 1 ^{*†}	139 \pm 8 ^{*†}	1.8 \pm 0.3 [*]
2	Antisense Ror1 (+80+97)	12	31 \pm 2 [*]	23 \pm 1 ^{*†}	130 \pm 7 ^{*†}	1.6 \pm 0.2 [*]
2	Antisense Ror2 (+24+41)	50	28 \pm 2 ^{*†}	24 \pm 1 ^{*†}	153 \pm 8 ^{*†}	1.4 \pm 0.9 [*]
2	Antisense Ror2 (+24+41)	25	28 \pm 2 ^{*†}	29 \pm 1 ^{*†}	130 \pm 10 [*]	1.5 \pm 0.2 [*]
2	Antisense Ror2 (+24+41)	12	32 \pm 2 ^{*†}	31 \pm 1 ^{*†}	109 \pm 7	1.6 \pm 0.2 [*]

E16 hippocampal cultures were plated at 75,000 cells/dish and allowed to develop for 1 (stage II) or 2 (stage III) days. Cells were fixed and stained with a tubulin antibody (clone DM1A). Neuritic processes from randomly selected cells were viewed by phase-contrast microscopy using a digital camera and traced onscreen. Neuritic length was determined using Metamorph Image Analysis Software. Sixty cells from three independent experiments were analyzed for each condition. Results are expressed as mean \pm s.e.m.

* $P < 0.01$ compared to measurements in the untreated control.

[†] $P < 0.01$ compared to measurements in the corresponding sense control.

Effect of the simultaneous downregulation of Ror1 and Ror2 by antisense oligonucleotides on neurite elongation in hippocampal neurons

Table 3

Days in culture	Treatment (oligonucleotide)	Dose (μ M)	Primary minor process length (μ m)	% Branched primary processes	Primary axon length (μ m)	Number of branches/axon
1	None	—	34 \pm 1	41 \pm 4	—	—
1	Sense Ror1+Sense Ror2	50	35 \pm 2	39 \pm 4	—	—
1	Antisense Ror1+Antisense Ror2	50	27 \pm 1*	24 \pm 3*	—	—
2	None	-	37 \pm 2	57 \pm 4	107 \pm 5	2.7 \pm 0.2
2	Sense Ror1+Sense Ror2	50	31 \pm 2*	50 \pm 4	112 \pm 3	2.2 \pm 0.2
2	Antisense Ror1+Antisense Ror2	50	26 \pm 1*	30 \pm 2*	165 \pm 8*	1.9 \pm 0.2 [†]

E16 hippocampal cultures were plated at 75,000 cells/dish and allowed to develop for 1 (stage II) or 2 (stage III) days. Cells were fixed and stained with a tubulin antibody (clone DM1A). Neuritic processes from randomly selected cells were viewed by phase-contrast microscopy using a digital camera and traced onscreen. Neuritic length was determined using Metamorph Image Analysis Software. Forty cells from three independent experiments were analyzed for each condition. Results are expressed as mean \pm s.e.m.

* $P < 0.01$ compared to all controls;

[†] $P < 0.01$ compared to untreated controls.